Equivalent Radii and Ratios of Radii from Solution Properties as Indicators of Macromolecular Conformation, Shape, and Flexibility

A. Ortega and J. García de la Torre*

Departamento de Química Física, Facultad de Química, Universidad de Murcia, 30071 Murcia, Spain

Received April 30, 2007

The equivalent radius for any solution property is the radius of a spherical particle having the same value of solution property as that of the macromolecule under consideration. Equivalent radii for different properties present a dependence on size and shape that are more similar than the values of the properties themselves. Furthermore, the ratios of equivalent radii of two properties depend on the conformation (shape or flexibility), but not on the absolute sizes. We define equivalent radii and their ratios, and describe their evaluation for some common models of rigid and flexible macromolecules. Using radii and ratios, we have devised procedures to fit macromolecular models to experimental properties, allowing the determination of the model parameters. Using these quantities, we can construct target functions for an equilibrated, unbiased optimization. The procedures, which have been implemented in public-domain computer programs, are illustrated for rigid, globular proteins, and the rodlike tobacco mosaic virus, and for semiflexible, wormlike heparin molecules.

1. Introduction

The size and the overall structure of macromolecules (eventually including flexibility) are traditionally determined from measurements of properties of dilute solutions. These include equilibrium properties, such as those derived from the scattering of electromagnetic radiation, and hydrodynamic properties, such as the sedimentation and diffusion coefficients and the solution viscosity. Modern techniques such as size exclusion chromatography with multiple detection (MD-SEC)[1] that permit the simultaneous measurement of various properties, including scattering, viscometry, molecular mass, and diffusion coefficient, even for the separate components of a heterogeneous mixture (see, for instance, refs 2−5), are enhancing interest in dilute solution properties as indicators of macromolecular size, shape, and flexibility.

For such structural elucidation in a general situation, experimental data of several properties are compared with results calculated from theoretical or computational approaches in order to find the structure that best fits the data. This general approach can be implemented in many different ways. For instance, the values of the various properties could be fitted individually or collectively to the predictions (i.e., seeking structural information for each property separately, or for all of them together). Alternatively, values of two properties can be combined to yield shape-dependent, dimensionless quantities that may facilitate the structural determination.

However, the way in which these ideas are implemented may produce important biases in the results or may somehow be inefficient. In the next two sections of this paper, we comment on more specific details and propose alternative procedures based on the equivalent radii for solution properties and the ratios of radii as effective and unbiased indicators of the overall structure of macromolecules in solution. In the subsequent section, we summarize the most commonly employed models for rigid and flexible macromolecules, namely, ellipsoids, cylinders, random coils, and wormlike chains, to which solution data are fitted (although the concepts of equivalent radii and their ratios are not model-specific and can be applied to any set of data, either from any model or from measurements). Our ultimate goal has been to devise robust criteria to fit model predictions to experimental data, implementing them in easy-to-use computational tools, Single-HYDFIT and Multi-HYDFIT. In the last two sections of the paper we respectively describe the mathematical details of these tools and examples of their applications.

2. Equivalent Radii

2.1. Motivation. Consider, as an illustrative example, the case of rodlike particles. For a rod of length L and diameter d, the properties change with dimensions mainly through powers of L (apart from a secondary influence on d that can be ignored for moderately small changes). Consider some common properties such as the radius of gyration, R_g, the translational diffusion coefficient, D_t, the intrinsic viscosity $[\eta]$, and the longest rotational time τ. From classical hydrodynamic theory of cylindrical particles, we know that the primary dependencies of properties on length are $R_g \propto L$, $D_t \propto L^{-1}$, $[\eta] \propto L^3$, and $\tau \propto L^3$. A difference in L of, say, 5% would produce a change of about 5% (increase and decrease, respectively) in R_g and D_t, but $[\eta]$ and τ would have an increase of about 16%. Any global fitting procedure aimed at determining the particle length, in which all the properties were given the same statistical importance, would give results more conditioned by the two latter properties. Of course, global multitechnique fitting approaches will in some way employ weights (see, for instance, the work of Nollmann et al.[6]). Nonetheless, it is desirable to devise a way to handle the properties that would avoid their different sensitivities to the structure, thus making weights unnecessary or using them for other purposes (like weighting for experimental errors).

* Corresponding author. Phone: Intnl - 34 968 367426. Fax: Intnl - 34 968 364148. E-mail: jgt@um.es.

10.1021/bm700473f CCC: $37.00
Published on Web 07/24/2007

Table 1. Expressions for the Equivalent Radii for Various Solution Properties

property	symbol	acronym	equivalent radii
translational friction coefficient	f_t	T	$a_T = f_t/6\pi\eta_0$
rotational relaxation times	τ	R	$a_R = (3kT/4\pi)^{1/3}(\tau/\eta_0)^{1/3}$
intrinsic viscosity	$[\eta]$	I	$a_I = (3/10\pi N_A)^{1/3}([\eta]M)^{1/3}$
covolume	u	C	$a_C = (3/32\pi)^{1/3}u^{1/3}$
volume	V	V	$a_V = (3/4\pi)^{1/3}V^{1/3}$
radius of gyration	R_g	G	$a_G = \sqrt{(5/3)}R_g$
longest chord	L	L	$a_L = L/2$

There are cases where similar biases could be introduced by some trivial but perhaps unnoticed facts; for example, for flexible polymers, the coil size can be expressed by the mean square radius of gyration, $\langle S^2\rangle$, which is the direct outcome of theories and scattering measurements, and, alternatively, a radius of gyration defined as $R_g = \langle S^2\rangle^{1/2}$. Clearly, any change gives a larger difference (at least twice as large) in $\langle S^2\rangle$ than in R_g. Thus, the way in which this property is employed in a multiproperty analysis may influence the outcome.

2.2. Definitions for Equivalent Radii. We propose a systematic form of expressing solution properties: the radius of the equivalent sphere, which is the sphere having the same value of that property. This idea has already been expressed and used in the literature for some properties, that is, the Stokes radius, which is the radius of a sphere having the same translational friction coefficient as the experimental system. We extend the concept to additional solution properties with unified notation. Actually, the properties that we consider are

- The translational friction coefficient, f_t, experimentally accessible from the diffusion coefficient D_t or the sedimentation coefficient s.
- The radius of gyration (or root-mean-squared (rms) radius of gyration, if the molecule is flexible), R_g, determined by radiation (light, X-ray, etc.) scattering.
- The intrinsic viscosity, $[\eta]$.
- A relaxation time, τ_x. This choice will depend on the case being considered. For rigid particles, there is a set of five ($x = 1, \cdots, 5$) rotational relaxation times.[7] These are usually observed from time- or frequency-dependent electro-optic or spectroscopy properties. For flexible-chain macromolecules, it is assumed that there is a long series of relaxation times, and this is also assumed for semiflexible macromolecules. For these cases, the quantity that is more easily accessible and the one that is observed on some molecular properties is the longest relaxation time, τ_1.
- The second virial coefficient, A_2 or B,[8] or, in the case of rigid particles, the covolume u (computable for arbitrary shapes[9]), which determines the concentration dependence of some solution properties.
- For rigid particles, the hydrodynamic volume, V. In some instances, particularly small globular proteins, this volume is related to the anhydrous volume $V_{anh} = M\bar{v}/N_A$, where $\bar{v}$ is the partial specific volume and N_A is Avogadro's number. The relationship is $V = V_{anh}(1 + \delta/\bar{v}\rho)$, where ρ is the solution density and δ is the degree of hydration expressed as grams of solvent (usually water in such cases) per gram of macromolecule. The consideration of solvation is essential for a precise determination of the size and shape of macromolecules or small or medium size, and to determine the hydrodynamic thickness of long fibrous or chain-like macromolecules. A consensus value $\delta = 0.3-0.4$ g/g can be used for both proteins[10] and nucleic acids.[11]
- The longest distance between any two points in the macromolecule, H. This quantity is usually determined for rigid macromolecules from the distribution of distances determined from the angular dependence of X-ray scattering intensities. For flexible-chain macromolecules, it could eventually be identified with the contour length or the length of the chain in its most extended conformation.

The equivalent radii are listed in Table 1. A single, capital letter (T, R, I, etc.) is used to denote the property, and the equivalent radius is denoted as a_X, with $X =$ T, R, I, and so forth.

As we describe below, the equivalent radii are not merely a different form of expressing the solution properties; they are the starting concept for constructing a formalism (and its implementation) based on these radii, or on the ratios of radii, which we introduce in the next section, for fitting properties to models for structural search or optimization. The formalism is aimed to treat jointly and simultaneously, in a properly balanced way, a set of various hydrodynamic coefficients and other quantities, which present diverse sensitivities to structural aspects or different ranges of experimental error. Experienced researchers could employ knowledge of the sensitivity of properties to size and shape, along with error propagation and other concepts, to devise valid fitting procedures. The equivalent radii, in addition to being instrumental for the design of our new optimization tools, also have the following (formal or practical) advantages:

(a) For a spherical particle, they all coincide with the geometric radius.

(b) For a particle of given, arbitrary shape, the radii depend on the particle size expressed as a linear dimension (not on its volume).

(c) The numerical values of the equivalent radii for the various properties are not much different from each other.

3. Ratios of Radii

3.1. Motivation. It is possible to formulate combinations of two solution properties that are dimensionless and do not depend on the size, but rather only the shape, of the macromolecular solute (for a rigid particle, the values for such combinations do not change in an uniform, isomorphous expansion).

In early, classical works,[12] the shape of rigid proteins was defined in terms of ellipsoidal models. For an ellipsoid of revolution, with axes ($2a$,$2b$,$2b$), the shape is entirely defined by the axial ratio $p = a/b$. Scheraga and Mandelkern[13] showed that a combination of f_t (or D_t, or s) with $[\eta]$, in the form of a dimensionless parameter

$$\beta = \frac{M^{1/3}[\eta]^{1/3}\eta_0}{100^{1/3}f_t} \qquad (1)$$

depends on p but not on the actual values of the dimensions, $2a$ and $2b$. The lowest bound for β is that for a spherical particle, $\beta = 2.112 \times 10^6$. For rigid macromolecules, it is also conventional, particularly for rigid macromolecules, to combine a solution property with the volume of the particle itself, or with a quantity directly derived from it. Thus, it is common practice to express the frictional coefficient of rigid structures as

$$P \equiv \frac{f_t}{f_{0,hyd}} = \frac{f_t}{6\pi\eta_0(3V/4\pi)^{1/3}} \tag{2}$$

where (in our notation) $f_{0,hyd}$ is the frictional coefficient of a sphere having the same hydrodynamic (hydrated or solvated) volume V as the particle. If solvation and other effects could be ignored, V is, in turn, deduced from M and the partial specific volume, $\bar{v}$, of the macromolecule, $V = \bar{v}M/N_A$. The term f/f_0 is sometimes denoted as P, after Perrin, since the expression of f for ellipsoids is attributed to this author.[14] A similar combination involves the intrinsic viscosity and molecular volume:

$$\nu = \frac{[\eta]}{\bar{v}} = \frac{[\eta]N_A}{M} \tag{3}$$

ν is also called the Einstein viscosity increment: for a sphere, the classical work of Einstein gave $\nu = 5/2$.[15] For ellipsoids, as studied by Simha,[16] $\nu(p)$ is a function of axial ratio.

In his classical work on the theory of polymer solution properties, Flory[17] showed that the following combination of the intrinsic viscosity $[\eta]$ with the radius of gyration, R_g,

$$\Phi = \frac{[\eta]M}{6^{3/2}R_g^3} \tag{4}$$

where M is the molecular weight, $R_g \sim \langle S^2\rangle^{1/2}$, and $\langle S^2\rangle$ is the mean square radius of gyration, should take a universal value for random-coil polymers that would be independent of molecular weight, local composition, structure, and so forth, depending only on solvent quality. Thus, it is accepted that, for every flexible-chain polymer in a Θ (ideal) solvent, there is a universal value of $\Phi = 2.5 \times 10^{23}$.[18] Flory[19] proposed a similar combination involving the translational friction coefficient (determined from the translational diffusion coefficient, D_t, or from the sedimentation coefficient, s):

$$P_0 = \frac{f_t}{6^{1/2}\eta_0 R_g} = \frac{kT}{6^{1/2}\eta_0 R_g D_t} \tag{5}$$

which, in the particular case of the flexible, randomly coiled macromolecule in the Θ state, takes the value $P_0 = 6.0$.[18,20] The quantities P_0 and Φ are not only applicable to flexible macromolecules. For instance, in the case of a rigid, compact spherical particle, it is easily found that $P_0 = 9.93$ and $\Phi = 9.23 \times 10^{23}$.

Since the 1950s, many other compound quantities have been proposed, involving a variety of solution properties, including those mentioned above and others, such as rotational coefficients, concentration-dependence constants, and so forth. For instance, compound quantities that combine the relaxation time with the intrinsic viscosity, $K_{\tau,\eta}$, and with the radius of gyration, K_{τ,R_g}, have been defined by Navarro et al.[21] For a more complete compilation, see, for instance, ref 22. Our motivation for reconsidering these compound quantities arises mainly from some of their inconveniences, such as the following:

(1) It is well-known that the various combinations present different sensitivities to the macromolecular shape. However, such sensitivity can be influenced by the definition itself. For instance, we recall the well-known insensitivity of the Scheraga Mandelkern parameter (β), which only changes from 2.11×10^6 to 2.63×10^6 (i.e., 19.7%) if the structure changes from a sphere to an elongated particle with an axial ratio of 17 (for instance, tobacco mosaic virus (TMV), *vide infra*), or to 2.32×10^6 for a random coil. However, if Scheraga and Mandelkern had defined their parameter as $\beta' = \beta^3 = M[\eta]\eta_0^3/(100f^3)$, involving the ratio $[\eta]/f^3$ rather than $[\eta]^{1/3}/f$, its sensitivity to shape would be greater, with β' going from 9.39×10^{18} for $p = 1$ to 16.39×10^{18} (a 42.7% change) for $p = 17$ in the above example.

(2) A related situation arises with regard to the sensitivity of the experimental errors. The error of a compound quantity is determined by the errors of the experimental measurements of the combined properties, according to the usual rules of propagation of errors. Following these rules, in the above example, the error in β' would be 3 times larger than that in β. Obviously, the study of shape sensitivity should be conducted considering error sensitivity as well, looking for those quantities that maximize the former and minimize the latter. The seemingly conflictive effects on the sensitivity to structure and the effect of experimental errors indicate the need of systematic and robust definitions of derived and compound quantities.

(3) Last, but not least, there is a noticeable variety in the notation employed for the compound quantities (Φ, P_0, β, P, ν, etc.) as well as in the numerical values that they adopt, for instance, in the limiting case of a spherical particle (9.23×10^{23}, 9.93, 2.112×10^6, 1, 2.5, etc.) or for other typical structures.

As we anticipated in the Introduction, we propose a new set of dimensionless, compound, shape-dependent quantities, namely, the ratios of equivalent radii, that have the same usefulness as the existing properties, but without their above-described inconveniences.

3.2. Definitions for Ratios of Radii. Now, we define the new compound quantities as ratios of the equivalent radii for a pair of properties. These ratios are denoted by a pair of capital letters, XY, indicating the properties involved in the order in which the quotient, a_X/a_Y, is calculated. For a given pair, this order is chosen so that the ratio is always greater that unity. In the Appendix, we give a list of these ratios. Here we list just a selection of them, expressing the compound quantity that they replace and its relationship to it:

$$XY \equiv a_X/a_Y \tag{6}$$

$$\mathrm{IT} \equiv \frac{a_I}{a_T} = \left(\frac{3[\eta]M}{10\pi N_A}\right)^{1/3}\frac{6\pi\eta_0}{f_t} = \left(\frac{30}{\pi N_A}\right)^{1/3}6\pi\beta \tag{7}$$

$$\mathrm{CT} \equiv \frac{a_C}{a_T} = \frac{6\pi\eta_0}{f}\left(\frac{3u}{32\pi}\right)^{1/3} = \left(\frac{81\pi^2}{4}\right)^{1/3}\psi^{1/3} \tag{8}$$

$$\mathrm{TV} \equiv \frac{a_T}{a_V} = \frac{f}{6\pi\eta_0(3V/(4\pi))^{1/3}} = P \tag{9}$$

$$\mathrm{TG} \equiv \frac{a_T}{a_G} = \frac{f}{6\pi\eta_0}\frac{\sqrt{3/5}}{R_g} = \frac{P_0}{\sqrt{10}\pi} \quad (10)$$

$$(\mathrm{RG})_x \equiv \frac{a_R}{a_G} = \left(\frac{3}{5}\right)^{1/2}\left(\frac{3kT\tau_x}{4\pi\eta_0}\right)^{1/3}\frac{1}{R_g} = \left(\frac{K_{\tau r,k}}{(K_{\tau r,k})_{sph}}\right)^{1/3} \quad (11)$$

4. Calculation of Equivalent Radii and Ratios

As indicated above, the calculation of the equivalent radii, and therefore their ratios, just requires the calculation of the properties themselves. In this section, we summarize the models and the theory and computational procedures available for such purpose.

4.1. Rigid Macromolecules with Simple Shapes: Ellipsoids and Cylinders. When the overall shape is compact or regular, as in the cases of globular proteins or helical structures, rigid macromolecules can be regarded, in a more or less simplified view, as particles with simple geometries, such as ellipsoids or cylinders. The ellipsoid of revolution is a classical model for the representation of globular proteins and other rigid biological macromolecules.[12] As mentioned above, the properties in solution of such ellipsoidal particles can be derived from the seminal works of Perrin,[14,23] Simha,[16] and Ishihara[24] (the calculation of other, simpler properties such as volume and radius of gyration are obvious). For the sake of simplicity, we restrict our study to axially symmetric ellipsoids, whose only shape parameter is the axial ratio p, although available theoretical results for triaxial ellipsoids[25,26] could easily be included.

Some macromolecules and macromolecular assemblies are better described by cylindrical shapes, ranging from disks to rods. Accurate results for the translational and rotational diffusion coefficients of rodlike macromolecules, in the significant range of axial ratios,[27−30] have been recently extended to the intrinsic viscosity[31] and covolume,[32] including cylinders with $p < 1$ (i.e., circular disks). Furthermore, for a cylinder of length L and diameter d, the volume, radius of gyration, and longest distance are, respectively, $V = \pi L d^2/4$, $R_g^2 = L^2/12 + d^2/8$ and $H = (L^2 + d^2)^{1/2}$. Thus, all the properties can be computed for a wide range of aspect ratios, $p = L/d$. The properties, and therefore the ratios or radii, are available for a wide range of p, from thin disks to moderately long rods. Longer rods are likely to be partially flexible, and they are better covered by the wormlike model (see below).

For revolution ellipsoids, cylinders, and any axially symmetric particle, there are two rotational friction coefficients, and the corresponding rotational diffusion coefficients, $D_r^{\parallel}$ and $D_r^{\perp}$, for rotation around the symmetry axis and a perpendicular axis, respectively. Rotational diffusion is observed in techniques such as NMR relaxation and time-dependent fluorescence anisotropy or electric birefringence. In these techniques, the time or frequency dependence is determined, for axially symmetric particles, by up to three rotational relaxation times, $\tau_a = (6D_r^{\perp})^{-1}$, $\tau_b = (5D_r^{\perp} + D_r^{\parallel})^{-1}$, and $\tau_c = (2D_r^{\perp} + 4D_r^{\parallel})^{-1}$. In various instances, only τ_a can be observed. Also, in other circumstances, one gets an overall correlation time, which is the harmonic mean of the five τ's (τ_b and τ_c are doubly degenerate), given by $\tau_h = [2(2D_r^{\perp} + D_r^{\parallel})]^{-1}$.

Figure 1 shows the equivalent radii of cylinders with diameter $d = 2$ nm and axial ratios from $p = 0.1$ (flat disk) to $p = 50$ (long rod). It is clear that all the a_X values for a given cylinder are of the same order of magnitude, and all the ratios of radii (which do not depend on the actual dimensions but only on p), take values not far from unity.

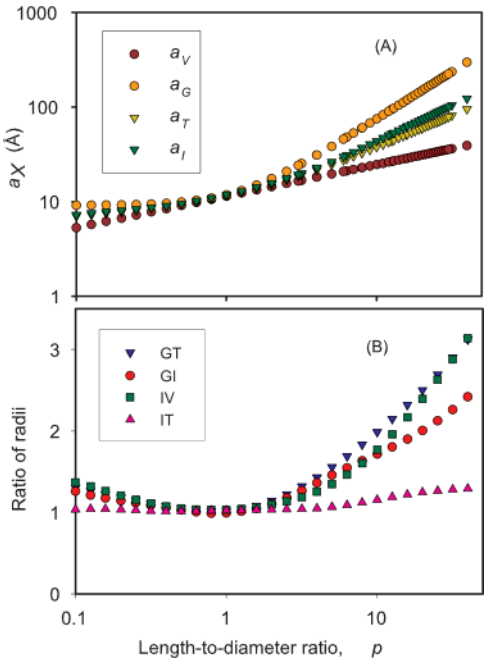

Figure 1. (A) Equivalent ratios for cylindrical particles with $d = 2$ nm (typical of double-helical B-DNA) as a function of the length-to-diameter ratio, $p = L/d$, calculated using the results in ref 31). (B) Some ratios of radii for cylindrical particles, ranging from rods with $p = 50$ to disks with $p = 0.1$.

4.2. Rigid Macromolecules of Arbitrary Shape. For macromolecules with arbitrarily complex shapes, the popular bead-model methodologies can be applied.[11,29,33−38] These procedures supply results for the various solution properties, from which the equivalent radii and the ratios of radii for such complex structures can be computed. The description of rotational diffusion for arbitrary shapes involves up to five relaxation times, τ_k, $k = 1, \cdots, 5$, and an harmonic mean or correlation time τ_h (also denoted τ_c) can also be formulated. So, in these cases, there are six choices for the rotational quantities but, for simplicity, this can be reduced to those based on τ_h, or in the longest τ_1. The most recent versions of HYDRO,[39] HYDROPRO,[35] and other programs of the HYDRO suite include the calculation of radii and ratios.

4.3. Flexible-Chain Macromolecules. Some of the classical universal functions, namely, the Flory constants Φ and P_0, were initially proposed for flexible-chain macromolecules. The first case that we distinguish here is that of flexible linear macromolecular chains in a Θ solvent. Recent, precise values for the Flory constants are $\Phi = 2.53 \times 10^{23}$ and $P_0 = 6.0$.[18,20] Other combinations involving the relaxation times are $K_{\tau\tau} = 1.8 \times 10^{24}$ and $K_{\tau\eta} = 0.50$.[21] Combining these values or relating them to those for a sphere, it is easy to obtain new values for some of our new dimensionless functions, which are indicated in Table 2.

We next consider linear chains in good solvent, with extreme excluded volume effects. Values of the Flory constants for this case are $\Phi = 1.9 \times 10^{23}$ and $P_0 = 5.3$.[40] In good solvent conditions, the second virial coefficient B is nonzero and can be used to calculate the molecular covolume and the functions associated with it. B is given by[8]

$$B = 4\pi^{3/2}N_A\frac{\langle S^2\rangle^{3/2}}{M^2}\Psi' \quad (12)$$

where Ψ' in the limit of very long chains in very good solvents

Table 2. Values of the Ratios of Radii for Flexible Chains

ratio	Θ solvent	good solvent
GI	1.53	1.69
GT	1.65	1.87
IT	1.08	1.11
GR	1.44	
IR	0.87	
TR	0.94	
GC		2.96
TC		1.58
IC		1.75

takes a limiting value, for which different theories give different numerical values. A recent, reliable result by Li et al.[41] is $\Psi' = 0.25$. (see also refs 42 and 43). Recalling that $B = uN_A/(2M^2)$, we express the covolume

$$u = 8\pi^{3/2}\langle S^2\rangle^{3/2}\Psi' \tag{13}$$

from which we immediately obtain the value for the ratio $GC = 2.96$. With regard to the relaxation times, unfortunately we do not have theoretical results in good solvents. With the previous results for P_0, Φ, and GC, we can obtain results for other ratios, which are listed in Table 2.

4.4. Semiflexible Macromolecules. This study of equivalent radii and ratios of radii can easily include macromolecules with partial flexibility. A common situation is that of filamentous molecules that can be described by the wormlike model, with a uniform flexibility measured by the persistence length, P (not to be confused with the Perrin function, here denoted with the same symbol, because the usual notations of these two quantities are identical). Actually, the conformation of the molecule is determined by the ratio of the contour length of the chain, L, to this intrinsic parameter. In addition to L and P, the properties of wormlike chains can have a marginal dependence on the thickness or diameter, d. The equivalent radii will depend on these three variables, and the ratios of radii will depend on only two, which can be chosen as L/P and d/L. For the evaluation of properties, radii, and ratios, various approaches and theories are available. In addition to the classical theories of Benoit and Doty[44] and Yamakawa and Fujii,[45,46] more recent calculations, mainly based on Monte Carlo simulations, that include the longest relaxation time, and more extreme values of L/P and d/L are available.[47,48]

The more complex but interesting case of macromolecules with segmental flexibility, having rigid subunits connected by more or less flexible joints, is amenable to hydrodynamic calculation using so-called rigid-body treatment, which combines Monte Carlo generation of conformations with rigid-body hydrodynamics for the calculation of properties.[49−51] This approach provides reasonable values for the translational coefficients and the intrinsic viscosity. The calculation of rotational (or, more properly, reorientational times) is also possible from Brownian dynamics simulation.[52] The referenced literature contains details on the procedures. Here we just wish to emphasize that it is feasible to predict equivalent radii and ratios of radii for such structures.

5. Conformational Search and Parameter Optimization with Radii or Ratios

As indicated above, equivalent radii and ratios can serve as indicators of the macromolecular conformation. The fact that all the properties are considered in a balanced manner, that the radii are of similar order of magnitude, and that the ratios are always not far from unity, for every conceivable macromolecular structure, allows us to design a robust method to investigate the macromolecular conformation from experimental data of solution properties. For all the experimentally available properties, a set of radii a_X and, subsequently, a set of ratios XY can be obtained. We now describe the proper way of comparing the experimental a_X and XY values with model calculations.

5.1. Conformational Search for a Single Structure. Suppose that we have data for some of the following properties: translational diffusion coefficient, D_t; sedimentation coefficient, s; intrinsic viscosity $[\eta]$; one of the relaxation times τ_x (usually the longest one, or perhaps the harmonic mean); the radius of gyration, R_g; the covolume u; and the volume of the hydrodynamic particle, V. From them, a set of equivalent radii, a_X, and eventually their ratios, can be evaluated and used as the source of information for a conformational search. The structural determination would typically be carried out on a trial-and-error basis, and more formally as an optimization procedure in which we seek to optimize the structure (dimensions and/or shape details) by minimizing the deviation of the values calculated for it from the experimental ones. This can be done in two ways: with ratios and with radii.

Using equivalent radii, the so-called target function to be minimized in the optimization takes the form

$$\Delta^2 = \Big(\sum_X w_X\Big)^{-1}\sum_X w_X\left[\frac{a_X(\mathrm{cal}) - a_X(\mathrm{exp})}{a_X(\mathrm{exp})}\right]^2 \tag{14}$$

Note that Δ^2 is the mean square relative deviation between the calculated and experimental equivalent radii. Such mean is a weighted average, over the available properties, X = D, S, R, I, G, V, and C. The equivalent radii a_D and a_S are the a_T values obtained from D_t and s, which can be included separately if these two properties have been measured independently (and the evaluation of a_S requires the value of M). Furthermore, we consider the possibility of assigning statistical weights, w_X, to the various properties. We recall that the use of equivalent radii gives similar importance to all the properties, and therefore statistical weights are not generally needed; that is, all the radii should be weighted identically. Anyway the user of this procedure may wish to give different importance to each data, perhaps in terms of the range of error or reliability of some experimental measurements.

If we are analyzing data for a single sample, there is also an alternative route based on the ratios of radii, which primarily determines the particle's shape, for instance, the parameter, p, instead of the two sizes L and d. For this we define another target function based on ratios:

$$\nabla^2 = \Big(\sum_{XY} w_{XY}\Big)^{-1}\sum_{XY} w_{XY}[XY(\mathrm{cal}) - XY(\mathrm{exp})]^2 \tag{15}$$

which is the mean square difference between the calculated and experimental ratios of radii. Note that, in eq 14, the right-hand side expression is divided by a_X(exp) because in that way the quotients are dimensionless and do not depend on molecular size, but in eq 15 we do not divide by XY(exp) because X and Y are already dimensionless quotients and very insensitive to size. The sum runs over all the ratios for the available pairs of properties, XY. Statistical weights w_{XY} could be optionally assigned to each pair. If weights are assigned to each property, a proper choice for the weight of the ratios is the harmonic mean, $w_{XY} = (1/w_X + 1/w_Y)^{-1}$. Otherwise, the weights can be

safely omitted. ∇^2 depends on the particle's shape instead of its dimensions; for instance, for ellipsoids and cylinders, it will be a function of the aspect ratio, p, only.

The expressions for Δ^2 in eq 14 and ∇^2 in eq 15 are of the form of a χ^2 deviation. The values to be reported will be the square roots, Δ and ∇. Thus, Δ is the rms difference between calculated and experimental equivalent radii, and 100Δ is a typical percent deviation, running over all properties and samples. Also ∇ is an rms deviation for the ratios of radii and serves as a significant indicator of the goodness of fit provided by the model. The use of eq 15 may simplify the optimization procedures, as it works with less information, that is, only with shape but not size. For instance, if we intend to characterize a cylindrical particle, in the first method we would face the minimization of a function of two variables, $\Delta(d,L)$, while in the second one we would have to minimize $\nabla(p)$, which is a function of only the aspect ratio p.

5.2. Case of Multiple Samples. The methodology can be extended to the case in which the structural search or the optimization of the structural parameters has to be carried out for a collection of samples. For this case, a generalization of the first procedure, based on equivalent radii seems adequate and simpler. The target function would be

$$\Delta^2 = \frac{1}{N_s}\sum_{i=1}^{N_s}\left[\left(\sum_X w_X\right)^{-1}\sum_X w_X\left(\frac{a_X(\text{cal}) - a_X(\text{exp})}{a_X(\text{exp})}\right)^2\right] \qquad (16)$$

where the outer summation runs over the N_s samples. Note that, in the definition of Δ^2, the use of the a_X values avoids the differences in the sensitivities of the various properties to the different particle dimensions of the successive samples. Also, in the case of a multisample analysis, the a_X values are larger for the larger molecules, and this is compensated by taking the relative deviation, $(a_X(\text{cal}) - a_X(\text{exp}))/a_X(\text{exp})$, so that the data for the larger molecules do not have a greater influence on Δ.

6. Applications

6.1. Single-HYDFIT and Multi-HYDFIT: Estimation of Structural Parameters for Ellipsoidal, Cylindrical, and Wormlike Macromolecules and Microparticles. For the determination of shape and size for an individual particle, we have implemented the concepts of equivalent radii and their ratios in a computer program, Single-HYDFIT, that considers simple hydrodynamic models, namely, the revolution ellipsoid, which has well-known theoretical results, and the cylinder, whose properties have been computed in our previous work.[31] The shape and size parameters of the model are evaluated fitting a series of experimental data of various solution properties. As mentioned above, the importance of the various properties in the optimization can be either balanced owing to the use of radii or ratios, or controlled by the user, introducing specific weights. The program works in the following modes:

- In modes E1 (for ellipsoids) and C1 (for cylinders), all the possible equivalent radii are evaluated from the experimental properties. Then the program attempts to find the dimensions and shape of the particle by minimization of the Δ^2 target function, as defined in eq 14. The parameters considered in the search are: (1) the aspect ratio, $p = L/d$ for cylinders or $p = a/b$ for ellipsoids, and (2) the length along the symmetry axis, that is, the length L of the cylinder, or the length of the distinct semiaxis, a. The other dimensions are evaluated *a posteriori*, as $d = L/p$ or $b = a/p$.
- In modes E2 (for ellipsoids) and C2 (for cylinders), the experimental properties are employed to evaluate all the possible ratios of radii. As these quantities depend only on the shape parameter p but not on the dimensions, the program searches the optimum of the target ∇, defined in eq 15, which is a function of only one variable, p. These modes, although less informative, may be computationally more efficient or accurate.

Another instance in which these concepts can be helpful in the determination of the overall structure and shape is when we have experimental data for a homologous series of samples (or fractions, in separation techniques) of the same molecule with varying molecular weight. The most frequent case is that of rodlike or wormlike macromolecules. For a series of samples of varying mass or length, the structural parameters common to all of them are the hydrodynamic diameter, d, the mass-per-unit length, $M_L = M/L$, and the persistence length, P. For this problem, we have developed another computer program, Multi-HYDFIT, which considers these three constants as adjustable parameters and tries to optimize the multisample Δ target function in eq 16. Here the minimization involves several variables. The optimizations can be unweighted, or, alternatively, the user can assign different weights to each property.

For the numerical minimization of a function of up to three variables, we have tried several procedures.[53] The Powell method[54] is rather efficient, but requires a good initial estimate. We have opted to employ, in a first stage, the simple grid procedure, in which an interval (lowest/highest limits) is indicated for each parameter, and a simple search for the absolute minimum is carried out giving equally spaced values to each parameter within its interval. Then, optionally, in a second stage, the minimum so found is refined by Powell minimization.

It may be interesting to know the uncertainty of the optimum values of the parameters arising from possible experimental errors. We have devised a simple procedure for the estimation of this uncertainty. Initially, typical values of the errors in experimental data are assigned for each property; for instance, *XM*% (say 5%) for M; *XG*% (say 5%) for R_g; *XS*% (say 3%), for s; *XD*% (say 3%), for D; *XI*% (say 8%) for $[\eta]$, and so forth. Then, the original experimental values are modified, adding "errors" that are random numbers with Gaussian distribution, so that the mean of the modified values is the original one, having a standard deviation equal to the above-mentioned typical error. Then, a full minimization (grid search followed by Powell refinement) with the modified experimental data is performed, obtaining values for the parameters. This is repeated a large number of times. The final values for each parameter are the averages of those obtained in all searches, and, consistently, the standard deviations are taken for the error bars.

The uncertainty in the fitted parameters can also be grasped from plots of the variation of the target functions, Δ or ∇, with the parameters near the minimum. Our programs provide files that can be imported to common graphics packages. The visualization (and the minimization itself) may be difficult when three parameters are involved. Nevertheless, we could fix one of the parameters, either because it is scarcely influential in the properties (this can be the case of the diameter of long rodlike or wormlike molecules) or because it has a value that is well defined by the known macromolecular structure (this may be so for M_L).

6.2. Tobacco Mosaic Virus. TMV is a macromolecular assembly composed by a single-stranded helical RNA surrounded by a capsid of single proteins, in which 16.3 identical subunits of the coat protein (per RNA helix turn) are inserted

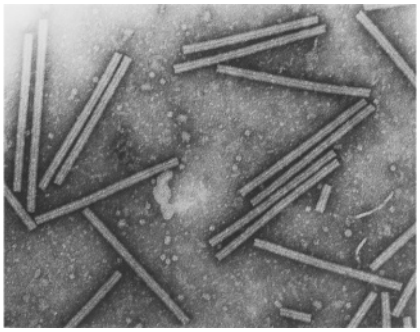

Figure 2. Micrograph of TMV clearly showing its cylindrical shape.

in a fashion similar to a spiral staircase. The structure is very stiff, the protein completely covers the RNA, and therefore the TMV particle really resembles a rigid rod. Indeed, electron micrographs (Figure 2) show clearly this picture, with a length and diameter of about 310 and 18 nm, respectively. Therefore this is a paradigmatic example of the application of the rodlike model, and its solution properties have been extensively studied to provide the information needed to test the theoretical and modeling work.

Using the set of consensus values for the various properties listed in Table 3, our global analysis Single-HYDFIT procedure for cylinders provides the aspect ratio and dimensions of the TMV rod. Mode C2, with p as the only parameter, and Mode C1, which fits both p and L, coincide in the value of $p = 16.6 \pm 1.6$. Indeed, a plot of ∇ versus p shows a well-defined minimum at this value, and the contour plot of Δ versus p and L (Figure 3) shows a minimum at this p and also gives the value of L. Thus the dimensions of TMV are finally obtained: $L = 318 \pm 7$ nm and $d = 17 \pm 2$ nm (averages of the two results in Table 3), which are in rather good agreement with those seen by electron microscopy. The minimum of the target function is $\Delta = 0.053$, which means that the rms relative difference between the experimental and calculated equivalent radii is about 5%. Indeed, Table 4 shows the comparison between experimental and fitted values for the equivalent radii and the ratios of radii. The differences are always smaller than 2%, except for the rotational diffusion coefficient, which is slightly smaller than the experimental value. If the D_r value is not included in the analysis, the resulting L, p, and d values are practically the same, and the fit is extremely good, with $\Delta = 0.019$. The fact that the observed rotational diffusion is faster than that predicted by calculation may be explained in terms of some degree of bending and torsional flexibilities (to which rotational diffusion is more sensitive than the other properties) that are not represented by the rigid cylinder. Even including D_r, the overall outcome is rather satisfactory, showing the performance of our

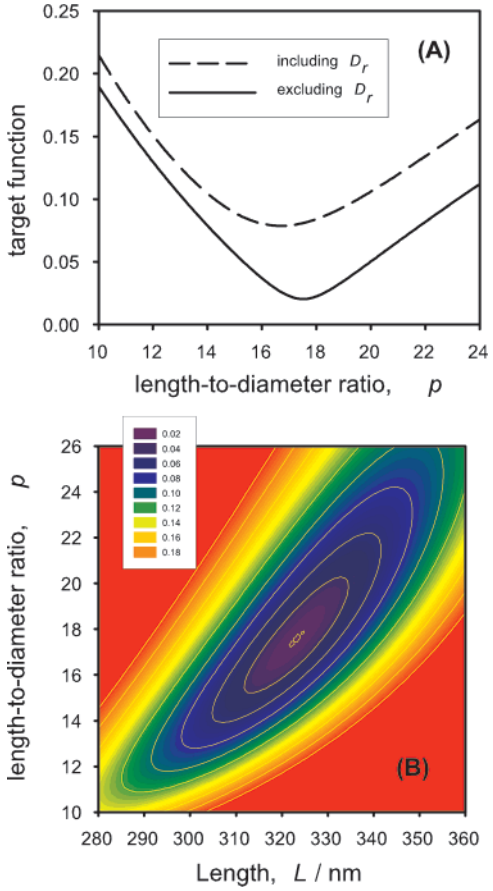

Figure 3. Plots of (A) ∇ and (B) Δ for the global analysis of TMV properties with the cylindrical model.

global analysis procedure and the good predictive capability of our equations[31] for cylinders.

6.3. Ellipsoidal Models for Globular Proteins. Apart from being the most direct and feasible extension of the hydrodynamic theory of spherical particles, the hydrodynamics of revolution ellipsoids has found a classical application in the description of solution properties of globular proteins, as described in elementary textbooks.[12,55] The possibility of calculating the hydrodynamic properties of proteins from the atomic-level structure by means of bead/shell models that closely reproduce the intricate details of the protein shape (e.g., using HYDRO-PRO[35]) makes the ellipsoidal model less necessary.

However, there are instances in which the ellipsoidal model may be useful. An evident situation is when atomic details of the macromolecule are not available or cannot be constructed, and one still needs to relate solution properties to an overall

Table 3. Values for TMV: Experimental Properties, Results from Single-HYDFIT for the Global Fitting, and Calculated Properties[a]

property	experimental	consensus	calculated
molecular weight, $M \times 10^6$	40,[a] 40.8[c]	40.4	
partial specific vol, $\bar{v}$, cm^3/g	0.73[c]	0.73	
radius of gyration, R_g, nm	85.6,[d] 93−113,[e] 92.4[a]	96	92
sedimentation coeff, s, S	188[a]	188	192
diffusion coeff, $D_t \times 10^8$, cm^2/s	4.30,[d] 4.50,[b] 4.19,[g] 4.27[c]	4.31	4.28
rotational diff. coeff, D_r, s^{-1}	312,[d] 318,[g] 287[h]	306	268
intrinsic viscosity, $[\eta]$, cm^3/g	36.7[a,e]	36.7	37.3

with D_r: $p = 16.6 \pm 1.6$, $\nabla = 0.068$, $L = 320 \pm 7$ nm, $\Delta = 0.053$
without D_r: $p = 17.1 \pm 1.4$, $\nabla = 0.021$, $L = 316 \pm 6$ nm, $\Delta = 0.019$

[a] Boedtker and Simmons (ref 66). [b] Fujime 1970 (ref 67). [c] Johnson and Brown (ref 68). [d] Kubota et al. (ref 69). [e] Newman and Swinney (ref 70). [f] Santos and Castanho (ref 71). [g] Wilcoxon and Schurr (ref 72). [h] Ermolina et al. (ref 73).

Table 4. Equivalent Radii (in nm) and Their Ratios for TMV, with Calculated Values of $L = 318$ nm and $d = 19$ nm

	experimental	calculated	Diff. %
a_T (D_t)	498	502	−0.9
a_T (s)	511	502	1.6
a_V	617	620	−0.5
a_G	1208	1210	−0.2
a_R	807	843	−4.4
IT (D_t)	1.239	1.232	0.5
IT (s)	1.208	1.232	−2.0
GT (D_t)	2.426	2.396	1.2
GT (s)	2.364	2.396	−1.3
GI	1.958	1.944	0.7
RI	1.340	1.369	4.5
GR	1.496	1.403	6.3
IR	1.958	1.921	1.8

(more or less elongated, or oblate, etc.) estimate of the particle's shape. Another utility of the ellipsoidal model is for coarse-grained modeling of nonglobular, multisubunit macromolecular structures. In the strategy implemented in the program MultiSUB (also known as crystallohydrodynamics[56]), the nearly globular domains or subunits are represented by cylinders or revolution ellipsoids. This simplification removes less necessary details and allows the analysis to concentrate on the more important aspect of global structure and arrangement of subunits. A recent example where this strategy is applied to determine the overall structure of antibodies has been reported by Lu et al.[57]

It is therefore convenient to have a procedure which could determine the optimum revolution ellipsoid of semiaxes a (single) and b (double), with axial ratio $p = a/b$ (>1 or <1 for prolate and oblate ellipsoids, respectively), that best reproduces the solution properties of the particle that is being modeled. In classical works this was achieved, for instance, by combining the translational friction coefficient from sedimentation or diffusion or from the intrinsic viscosity with the molecular covolume, somehow expanded to include hydration. Such analysis was done in terms of the "named" (nonsystematic) combinations that are functions of p, like the Perrin[14] and Simha functions,[16] and others that have been proposed more recently.[58] With the global-modeling methodology that we have presented in this work, the determination of the best-fitting ellipsoid can be made in a systematic manner, simultaneously analyzing data for the various solution properties, using the Single-HYDFIT procedure.

There may be situations in which experimental data for the solution properties are not available (for instance, when a domain or subunit cannot be characterized separately), but one instead has access to an atomic structure. If an optimized ellipsoid is needed for such species, we propose a strategy based on HYDROPRO, which can be used to estimate a set of "synthetic" values of many solution properties, calculated with this program with the standard value of the hydrodynamic radius of the atoms (about 3.2 Å), which accounts well for the typical hydration of globular proteins. The results from HYDROPRO would be the data given to Single-HYDFIT, which would find the ellipsoid that best fits the properties previously calculated for the atomic model.

As an example of these situations, we consider a typical and well-characterized protein for which experimental data are abundant: hen egg white lysozyme. With the data compiled by us in previous work[10,35] and those in another recent, comprehensive compilation by Rai et al.,[59] we adopt the following

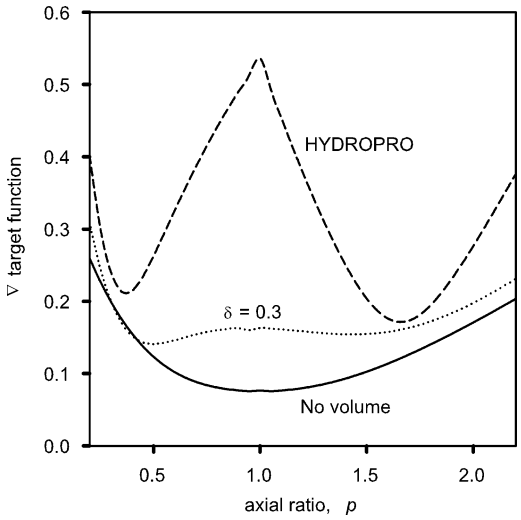

Figure 4. Plot of ∇ vs p for the ellipsoidal model of lysozyme for various sets of properties: experimental without and with hydrated volume, and HYDROPRO values.

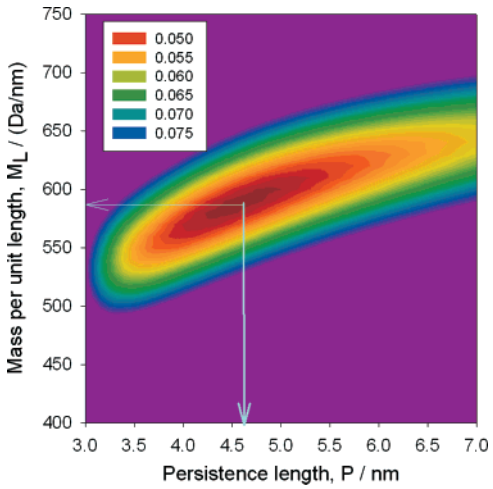

Figure 5. Contour plot of the target function Δ, for the wormlike chain model of heparin, as a function of the persistence length and mass per unit length (the d parameter is fixed to its optimum value, 1.1 nm).

compromise values for the following five solution properties: $D_t = 1.09 \times 10^{-6}$ cm^2/s, $s = 1.89$ S, $R_g = 14.6$ Å, $[\eta] = 3.3$ cm^3/g, $\tau_1 = 8.4$ ns (harmonic mean or correlation time). The analysis of s and $[\eta]$ requires additional values $M = 14320$ Da and $\bar{v} = 0.71$ cm^3/g. Combining the five properties in a Single-HYDFIT analysis, we find that the best shape corresponds to $p \approx 1$, that is, to a spherical particle, which is in contrast with the well-known, clearly nonspherical shape of the protein. It is interesting to look at the plot of ∇^2 versus p (Figure 4) and the contour plots of Δ^2 versus p and a (not shown), where we observe a single but rather wide minimum.

In this first attempt, the volume of the particle has not been considered as an independent property. However, it is known that greatest sensitivity to shape is for the combinations that involve a solution property and the particle's (hydrated) volume. This volume can be estimated from $M = 14320$ Da and $\bar{v} = 0.71$ cm^3/g and a reasonable guess for hydration of typically $\delta = 0.3$ grams of water per gram of protein, which yields $V = 2.41 \times 10^{-20}$ cm^3. When this value is included in the analysis, we get the results plotted in Figure 4. Now there are two minima of practically the same depth, one at $p = 0.5$ and another at p

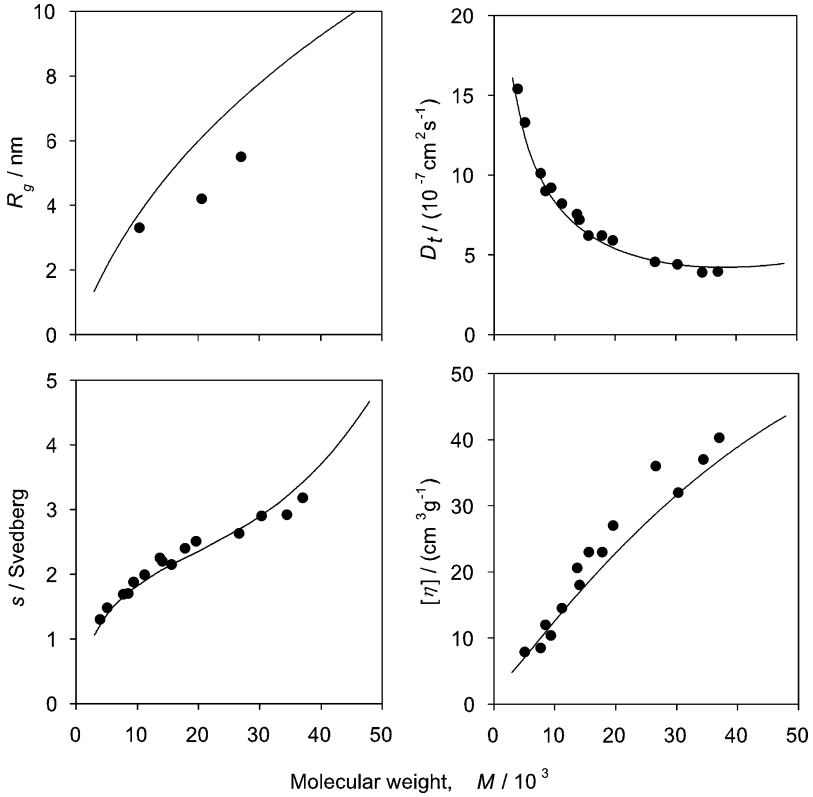

Figure 6. Comparison of the experimental values with those calculated with the optimum parameters for the four properties of all the heparin samples.

= 1.5. This situation is reminiscent of the classical analysis of protein shapes using ellipsoids: there is an ambiguity between an oblate shape and a prolate one. As described in textbooks by Tanford[12] and Van Holde,[60] given the value of a compound quantity combining two solution properties, there are two solutions for the ellipsoid axial ratio: one prolate with $p > 1$ and one oblate with $p < 1$. When, years ago, low-resolution crystallographic data were available, they were employed to choose one of the options. Now combining two or more solution properties, as we do in our procedure, the fit for one of the cases is just very slightly, perhaps insignificantly, better. Then, we also recall the crystallographic structure, which indicates a prolate shape with p close to 1.5, which is one of the solutions found by Single-HYDFIT.

Then, we consider the alternative of using the data predicted by HYDROPRO. Again, the visualization of the plots (Figure 4) shows two minima, the absolute one now for $p = 1.7$ (prolate), and the secondary one for $p = 0.5$. It is clear that, in addition to the absolute minimum, which is the primary result of HYDFIT, the dependence of the target function on the values of the parameters should be examined, looking for other possible local minima.

As mentioned above, ambiguities in the optimization can be resolved with structural information. In other studies where the globular proteins had to be represented by ellipsoids, a strategy based on the moments of inertia (which are good indicators of the distribution of mass) has been employed. This was done, for instance, in early crystallohydrodynamic works[56] representing proteins by ellipsoids with equalized moments of inertia. Another example was in the efficient calculation of NMR residual dipolar couplings based on revolution ellipsoids, as implemented in program ORIEL.[61] We employ here this strategy, which consists of the following basic steps: (1) Obtain the gyration tensor (equivalent to the inertial tensor) from the atomic coordinates. (2) Diagonalize this tensor to obtain the eigenvalues, G_1, G_2 and G_3. (3) Examine the possible pairs of these three values to find the pair in which the values are more similar. Take the mean of that pair as G_a, and the remaining one would be G_b. (4) For a revolution ellipsoid with semiaxes a, a, and b, the eigenvalues of the gyration tensor must be $a^2/5$ (duplicate) and $b^2/5$, which, when equated to the numerical values, give the values of a and b. Following these steps for lysozyme, the results are $G_1 = 48.5$ Å^2, $G_2 = 40.2$ Å^2 and $G_3 = 112.2$ Å^2, with $G_a = 44.3$ Å^2 and $G_b = 112.2$ Å^2, from which, finally, $a = 23.7$ Å and $b = 14.9$ Å, so that $p = 1.59$, in good agreement with the dimension predicted by one of the minima detected by our hydrodynamic fitting procedure. We propose that this method should be employed to solve possible ambiguities, i.e., make a choice between prolate and oblate alternatives. Once the best choice is made, the values derived from Single-HYDFIT should be preferred, as they correspond to the best fit of the hydrodynamic behavior, which is what is pursued for further hydrodynamic applications.

6.4. Heparin. As an example of the application of the optimization procedures to a typical wormlike macromolecule in a multisample case, we describe the determination of the wormlike-chain parameters of heparin. This polysaccharide, whose more important physiological functions appear to be that of an antithrombotic and anticoagulant agent, presents variable length and composition. The number of uronic acid residues, and therefore the molecular weight, vary from one fraction to another, making it a perfect candidate for our application Multi-HYDFIT.

The experimental study of the solution properties of heparin recently reported by Pavlov et al.[62] provides an excellent source of data to show the applicability of our concepts and methodology. These authors measured four properties—diffusion coefficient (D_t), sedimentation coefficient (s), intrinsic viscosity ([η])

and radius of gyration (R_g)—of 15 well-defined heparin fractions, with molecular weights in the range of $3.9-37 \times 10^3$. The availability of data for such a large collection of polymers of varying length is a guaranty of the quality of the resulting parameters. They analyzed their data in a detailed but rather labored manner, by means of property-specific procedures, with the hydrodynamics of the wormlike chain described by the Yamakawa−Fujii theory.

Employing our results and methodology, the application of the program for global analysis Multi-HYDFIT to the heparin data of Pavlov et al. immediately yields the values for the molecular wormlike parameters: $d = 1.1 \pm 0.3$ nm, $P = 4.6 \pm 0.4$ nm, and $M_L = 590 \pm 20$ Da/nm. The minimum value of Δ is 0.05, which indicates a typical 5% difference between calculation and experiments for all the samples and properties. The dependence of the target function on the model parameters is depicted in Figure 5 where, in order to make the function depend on only two variables, the hydrodynamic diameter has been fixed at its optimum value. Actually, such plots serve as an indicator of the sensitivity of the fit to P and M_L. The valley in the contour plot is appreciably narrower in the direction of M_L than in that of P. Thus, the uncertainty in P is larger than that in M_L, and this finding is corroborated independently by another aspect of our procedure, that is, the simulation of errors in the parameters associated with uncertainties in experimental data.

The goodness of the fit can be judged looking at plots of properties versus molecular weight, which are presented in Figure 6. We note that the R_g values of two of the samples are overestimated, and the $[\eta]$ of a few samples is underestimated, with excellent agreement for D_t and s. As indicated above, the difference between experimental and calculated values is always only a few percent. Thus, this example shows how the optimization procedures based on equivalent radii and their implementation in our computer algorithms permit a robust, unbiased, and efficient determination of macromolecular parameters, in the rather complex case of the three-parameter wormlike model applied to various properties of many samples of this biological macromolecule.

6.5. Other Applications. Solution properties, either experimental or calculated, for any model can be transformed into equivalent radii and ratios of radii. Therefore, the values of Δ and ∇ can be used to quantify to what extent an assumed structure or a set of structural parameters conform with experimental data of solution properties. Our programs of the HYDRO suite allow the calculation of properties from given structures in a variety of situations. We have devised an interface such that Single-HYDFIT can read the results generated for multicase executions of the HYDRO programs (using our MultiHYDRO[63] and MultiSUB[64] or similar tools) with multiple structures, and find the one that minimizes the Δ or ∇ target functions.

The global, multiproperty and multisample capacities of Multi-HYDFIT with our implementation of the wormlike chain model open the possibility of analyzing in an easy, systematic, and accurate manner solution properties, for the determination of the diameter, mass-to-length ratio, and persistence length of a number of synthetic and biological polymers that are customarily characterized by MD-SEC. Polysaccharides are good examples of such possibilities. Programs that would put the outcome of MD-SEC instruments into the form of Multi-HYDRO input files can be easily written for that purpose.

7. Computer Programs

Programs Single-HYDFIT and Multi-HYDFIT are of public domain, and can be downloaded from our Web site, http://leonardo.fcu.um.es/macromol/.

Acknowledgment. This work was supported by grant CTQ-2006-06831 from Ministerio de Educacion y Ciencia (MEC), including FEDER funds. A.O. acknowledges fellowships from MEC and Caja Murcia.

Appendix

The following is a list of the definitions of the ratios of equivalent radii:

$$(\mathrm{TR})_x \equiv \frac{a_T}{a_R} = \frac{f_t}{6\pi\eta_0}\left(\frac{4\pi\eta_0}{3kT\tau_x}\right)^{1/3} = P\left(\frac{\tau_0}{\tau_x}\right)^{1/3} = \Psi_x \quad (17)$$

$$\mathrm{IT} \equiv \frac{a_I}{a_T} = \left(\frac{3[\eta]M}{10\pi N_A}\right)^{1/3}\frac{6\pi\eta_0}{f_t} = \left(\frac{30}{\pi N_A}\right)^{1/3} 6\pi\beta = \frac{\beta}{\beta_{sph}} \quad (18)$$

$$\mathrm{CT} \equiv \frac{a_C}{a_T} = \frac{6\pi\eta_0}{f}\left(\frac{3u}{32\pi}\right)^{1/3} = \left(\frac{81\pi^2}{4}\right)^{1/3}\psi^{1/3} = \left(\frac{\psi}{\psi_{sph}}\right)^{1/3} \quad (19)$$

$$\mathrm{TV} \equiv \frac{a_T}{a_V} = \frac{f}{6\pi\eta_0(3V/(4\pi))^{1/3}} = P \quad (20)$$

$$\mathrm{TG} \equiv \frac{a_T}{a_G} = \frac{f}{6\pi\eta_0}\frac{\sqrt{3/5}}{R_g} = \frac{P_0}{\sqrt{10}\pi} = \frac{P_0}{(P_0)_{sph}} \quad (21)$$

$$\mathrm{TL} \equiv \frac{a_T}{a_L} = \frac{f}{3\pi\eta_0 L} \quad (22)$$

$$(\mathrm{IR})_x \equiv \frac{a_I}{a_R} = \left(\frac{2[\eta]M\eta_0}{5N_A kT_{\tau x}}\right)^{1/3} = \left(\frac{2\Lambda_x}{5}\right)^{1/3} = \left(\frac{\Lambda_x}{(\Lambda_x)_{sph}}\right)^{1/3} \quad (23)$$

$$(\mathrm{RC})_x \equiv \frac{a_R}{a_C} = \left(\frac{8kT\tau_x}{\eta_0 u}\right)^{1/3} \quad (24)$$

$$(\mathrm{RV})_x \equiv \frac{a_R}{a_V} = \left(\frac{kT\tau_x}{\eta_0 V}\right)^{1/3} = \left(\frac{\tau_x}{\tau_0}\right)^{1/3} \quad (25)$$

$$(\mathrm{RG})_x \equiv \frac{a_R}{a_G} = \left(\frac{3}{5}\right)^{1/2}\left(\frac{3kT\tau_x}{4\pi\eta_0}\right)^{1/3}\frac{1}{R_g} = \left(\frac{K_{tr,x}}{(K_{tr,x})_{sph}}\right)^{1/3} \quad (26)$$

$$(\mathrm{RL})_x \equiv \frac{a_R}{a_L} = \left(\frac{6kT\tau_x}{\pi\eta_0 L^3}\right)^{1/3} \quad (27)$$

$$\mathrm{CI} \equiv \frac{a_\mathrm{C}}{a_\mathrm{I}} = \left(\frac{10uN_\mathrm{A}}{32[\eta]M}\right)^{1/3} = \left(\frac{\Pi}{(\Pi)_\mathrm{sph}}\right)^{1/3} \tag{28}$$

$$\mathrm{IV} \equiv \frac{a_\mathrm{I}}{a_\mathrm{V}} = \left(\frac{2[\eta]M}{5VN_\mathrm{A}}\right)^{1/3} = \left(\frac{\nu}{\nu_\mathrm{sph}}\right)^{1/3} \tag{29}$$

$$\mathrm{IG} \equiv \frac{a_\mathrm{I}}{a_\mathrm{G}} = \left(\frac{3[\eta]M}{10\pi N_\mathrm{A}}\right)^{1/3}\left(\frac{3}{5}\right)^{1/2}\frac{1}{R_\mathrm{g}} = \left(\frac{\Phi}{\Phi_\mathrm{sph}}\right)^{1/3} \tag{30}$$

$$IL \equiv \frac{a_I}{a_L} = \left(\frac{12[\eta]M}{5\pi N_\mathrm{A}L^3}\right)^{1/3} \tag{31}$$

$$CV \equiv \frac{a_C}{a_V} = \left(\frac{u}{8V}\right)^{1/3} = \left(\frac{u_\mathrm{red}}{(u_\mathrm{red})_\mathrm{sph}}\right)^{1/3} \tag{32}$$

$$CG \equiv \frac{a_C}{a_G} = \left(\frac{3u}{32\pi}\right)^{1/3}\left(\frac{3}{5}\right)^{1/2}\frac{1}{R_\mathrm{g}} \tag{33}$$

$$CL \equiv \frac{a_C}{a_L} = \left(\frac{3u}{4\pi L^3}\right)^{1/3} \tag{34}$$

$$GV \equiv \frac{a_G}{a_V} = \left(\frac{4\pi}{3V}\right)^{1/3}\left(\frac{5}{3}\right)^{1/2}R_\mathrm{g} = \left(\frac{G}{G_\mathrm{sph}}\right)^{1/3} \tag{35}$$

$$VL \equiv \frac{a_V}{a_L} = \left(\frac{6V}{\pi L^3}\right)^{1/3} \tag{36}$$

$$LG \equiv \frac{a_L}{a_G} = \left(\frac{3}{20}\right)^{1/2}\frac{L}{R_\mathrm{g}} = \frac{H}{H_\mathrm{sph}} \tag{37}$$

In eqs 17−37, we relate our ratios of axial ratios to other dimensionless, compound quantities that have been described in the literature. As mentioned above, P_0, Φ, and β are the Flory and Scheraga−Mandelkern parameters, P is the Perrin factor, and ν is the Einstein viscosity increment. $K_{\tau,r}$ and H are defined in refs 21 and 9, respectively, and Ψ, ψ, Λ, ϕ, u_red, and G are defined in either ref 25 or ref 65.

References and Notes

(1) *Multiple Detection in Size Exclusion Chromatography*; Striegel, A. M., Ed.; Oxford University Press: Oxford, 2004.
(2) Hartman, W. K.; Saptharishi, N.; Yang, X.; Mitra, G.; Soman, G. *Anal. Biochem.* **2004**, *325*, 227−239.
(3) Sun, T.; Chance, R.; Graesley, W.; Lohse, D. J. *Macromolecules* **2004**, *37*, 4304−4312.
(4) Yanagisawa, M.; Isogai, A. *Biomacromolecules* **2005**, *6*, 1258−1265.
(5) Vold, I. M. N.; Kristiansen, K. A.; Christensen, B. E. *Biomacromolecules* **2006**, *7*, 2136−2146.
(6) Nollmann, M.; Stark, W.; Byron, O. *J. Appl. Crystallogr.* **2005**, *38*, 874−887.
(7) Favro, L. D. *Phys. Rev.* **1960**, *119*, 53−62.
(8) Yamakawa, H. *Modern Theory of Polymer Solutions*; Harper & Row: New York, 1971.
(9) García de la Torre, J.; Harding, S.; Carrasco, B. *Eur. Biophys. J.* **1999**, *28*, 119−132.
(10) García de la Torre, J. *Biophys. Chem.* **2001**, *93*, 150−159.
(11) Fernandes, M.; Ortega, A.; López Martínez, M.; García de la Torre, J. *Nucleic Acids Res.* **2002**, *30*, 1782−1788.
(12) Tanford, C. *Physical Chemistry of Macromolecules*; J. Wiley and Sons: New York, 1961.
(13) Scheraga, H.; Mandelkern, L. *J. Am. Chem. Soc.* **1953**, *75*, 179−184.
(14) Perrin, F. *J. Phys. Radium* **1936**, *7*, 1−11.
(15) Einstein, A. *Ann. Phys.* **1906**, *19*, 289−306 (English translation in *Investigation on the Theory of the Brownian Movement*; Dover: New York, 1956).
(16) Simha, R. *J. Phys. Chem.* **1940**, *44*, 25−34.
(17) Flory, P., Jr.; T. G. F. *J. Am. Chem. Soc.* **1951**, *73*, 1904−1908.
(18) García de la Torre, J.; López Martínez, M.; Tirado, M.; Freire, J. *Macromolecules* **1984**, *17*, 2715−2722.
(19) Flory, P. *Principles of Polymer Chemistry*; Cornell University Press: Ithaca, NY, 1953.
(20) Freire, J.; Rey, A.; García de la Torre, J. *Macromolecules* **1986**, *19*, 457−462.
(21) Navarro, S.; López Martínez, M.; García de la Torre, J. *J. Chem. Phys.* **1995**, *103*, 7631−7639.
(22) Harding, S.; Cölfen, H. *Anal. Biochem.* **1995**, *228*, 131−142.
(23) Perrin, F. *J. Phys. Radium* **1934**, *5*, 497−511.
(24) Isihara, A. *J. Chem. Phys.* **1950**, *18*, 1446−1449.
(25) Harding, S. *Biophys. Chem.* **1995**, *55*, 69−93.
(26) Harding, S.; Dampier, M.; Rowe, A. *Biophys. Chem.* **1982**, *15*, 205−208.
(27) Tirado, M.; García de la Torre, J. *J. Chem. Phys.* **1979**, *71*, 2581−2587.
(28) Tirado, M.; García de la Torre, J. *J. Chem. Phys.* **1980**, *73*, 1968−1993.
(29) García de la Torre, J.; Bloomfield, V. *Q. Rev. Biophys.* **1981**, *14*, 81−139.
(30) García de la Torre, J.; López Martínez, M.; Tirado, M. *Biopolymers* **1984**, *23*, 611−615.
(31) Ortega, A.; García de la Torre, J. *J. Chem. Phys.* **2003**, *119*, 9914−9919.
(32) Ortega, A.; de la Torre, J. G. *J. Am. Chem. Soc.* **2005**, *127*, 12764−12765.
(33) García de la Torre, J.; Bloomfield, V. *Biopolymers* **1977**, *16*, 1747−1763.
(34) Carrasco, B.; García de la Torre, J. *Biophys. J.* **1999**, *76*, 3044−3057.
(35) García de la Torre, J.; Huertas, M.; Carrasco, B. *Biophys. J.* **2000**, *78*, 719−730.
(36) García de la Torre, J.; Huertas, M.; Carrasco, B. *J. Magn. Reson.* **2000**, *147*, 138−146.
(37) García de la Torre, J.; Llorca, O.; Carrascosa, J.; Valpuesta, J. *Eur. Biophys. J.* **2001**, *30*, 457−462.
(38) García de la Torre, J. *Biophys. Chem.* **2001**, *94*, 265−274.
(39) García de la Torre, J.; Navarro, S.; López Martínez, M.; Díaz, F.; López Cascales, J. *Biophys. J.* **1994**, *67*, 530−531.
(40) García Bernal, J.; Tirado, M.; García de la Torre, J. *Macromolecules* **1991**, *24*, 593−598.
(41) Li, B.; Madras, N.; Sokal, A. *J. Stat. Phys.* **1995**, *80*, 661−754.
(42) Rubio, A.; Freire, J. *Macromolecules* **1996**, *29*, 6946−6951.
(43) Rubio, A.; Freire, J. *J. Chem. Phys.* **1997**, *106*, 5638−5647.
(44) Benoit, H.; Doty, P. *J. Phys. Chem.* **1953**, *57*, 958−963.
(45) Yamakawa, H.; Fujii, M. *Macromolecules* **1974**, *7*, 128−135.
(46) Yamakawa, H.; Fujii, M. *Macromolecules* **1974**, *7*, 649−654.
(47) Hagerman, P.; Zimm, B. *Biopolymers* **1981**, *20*, 1481−1502.
(48) García Molina, J.; López Martínez, M. C.; García de la Torre, J. *Biopolymers* **1990**, *29*, 883−900.
(49) García de la Torre, J.; Jiménez, A.; Freire, J. *Macromolecules* **1982**, *15*, 148−154.
(50) Iniesta, A.; Díaz, F.; García de la Torre, J. *Biophys. J.* **1988**, *54*, 269−275.
(51) García de la Torre, J. *Eur. Biophys. J.* **1994**, *23*, 307−322.
(52) García de la Torre, J.; Pérez Sánchez, H.; Ortega, A.; Hernández Cifre, J.; Fernandes, M.; Díaz Baños, F.; López Martínez, M. *Eur. Biophys. J.* **2003**, *32*, 477−486.
(53) Press, W.; Flannery, B.; Teukolsky, S.; Vetterling, M. T. *Numerical Recipes: The Art of Scientific Computing*; Cambridge University Press: Cambridge, 1986.
(54) Brent, R. *Algorithms for Minimization without Derivatives*; Prentice Hall: Englewood Cliffs, NJ, 1986.
(55) van Holde, K. E.; Johnson, W. C.; Ho, P. S. *Physical Biochemistry*; Prentice Hall: New York, 2002.
(56) Carrasco, B.; García de la Torre, J.; Byron, O.; King, D.; Walters, C.; Jones, S.; Harding, S. *Biophys. J.* **1999**, *77*, 2902−2910.
(57) Lu, Y.; Longman, E.; Davis, K.; Ortega, A.; Grossmann, J.; Michaelsen, T.; de la Torre, J. G.; Harding, S. *Biophys. J.* **2006**, *91*, 1688−1697.
(58) Harding, S. *Biochem. J.* **1980**, *189*, 359−361.
(59) Rai, N.; Nollmann, M.; Spotorno, B.; Tassara, G.; Byron, O.; Rocco, M. *Structure* **2005**, *13*, 723−734.
(60) van Holde, K. *Physical Biochemistry*; Prentice Hall: Englewood Cliffs, NJ, 1971.

(61) Fernandes, M.; Bernado, P.; Pons, M.; García de la Torre, J. *J. Am. Chem. Soc.* **2001**, *123*, 12037−12047.
(62) Pavlov, G.; Finet, S.; Tatarenko, K.; Korneeva, E.; Ebel, C. *Eur. Biophys. J.* **2003**, *32*, 437−449.
(63) García de la Torre, J.; Ortega, A.; Sánchez, H. P.; Cifre, J. H. *Biophys. Chem.* **2005**, *116*, 121−128.
(64) García de la Torre, J.; Carrasco, B. *Biopolymers* **2002**, *63*, 163−167.
(65) García de la Torre, J.; Carrasco, B.; Harding, S. E. *Eur. Biophys. J.* **1997**, *25*, 361−372.
(66) Boedtker, H.; Simmons, N. *J. Am. Chem. Soc.* **1958**, *80*, 2550−2556.
(67) Fujime, S. *J. Phys. Soc. Jpn.* **1970**, *29*, 416.
(68) Johnson, P.; Brown, W. In *Laser Light Scattering in Biochemistry*; Harding, S. E.; Sattelle, D. B.; Bloomfield, V. A., Eds.; Royal Society of Chemistry: Cambridge, U.K., 1992: pp 161−183.
(69) Kubota, K.; Urabe, H.; Tominaga, Y.; Fujime, S. *Macromolecules* **1984**, *17*, 2096.
(70) Newman, J.; Swinney, H. L. *Biopolymers* **1976**, *15*, 301−315.
(71) Santos, N.; Castanho, M. *Biophys. J.* **1996**, *71*, 1641−1650.
(72) Wilcoxon, J.; Schurr, J. M. *Biopolymers* **1983**, *22*, 849−867.
(73) Ermolina, I.; Morgan, H.; Green, N.; Milner, J. J.; Y. F. *Biochim. Biophys. Acta* **2003**, *1622*, 57−63.

BM700473F